10

Magnetic Irreversibility and Resistive Transition in YBaCuO Superconductors: Interpretations and Possible Correlations

Fábio Teixeira Dias
Universidade Federal de Pelotas
Brazil

1. Introduction

The second generation of high-temperature superconductors (HTSC) have been extensively studied since the discovery. Because of the potential for technological applications several research groups around the world have studied the electric and magnetic properties of HTSC that can provide important information about the performance of these materials when, e.g., magnetic fields are applied in many different applications.

This chapter will be dedicated to describe the main results obtained with YBaCuO superconductors and the interpretations on the resistive transition and magnetic irreversibility limit with special attention to their correlations. It will be presented experimental results obtained by magnetization and magnetotransport measurements in several magnetic field regimes with the purpose of disclosing the connection between the magnetic irreversibility limit and the zero resistance temperature as a function of applied magnetic field.

The discussion will be centered in experimental evidences obtained not only in pure YBaCuO materials but also in doped materials. It will be presented results obtained with single crystals, poly-crystals (sintered and melt-textured) and thin film materials grown by different techniques aiming to discuss the influence of the microstructure in the electric and magnetic properties.

Initially it will be done a rapid review about the YBaCuO superconductor and its basic properties, with special attention to magnetic and electric properties, such as magnetic irreversibility and resistive transition.

The next topic to be approached is the central theme proposed in this chapter i.e. the correlation between the magnetic irreversibility and the zero resistance in YBaCuO superconductors and the subsequent fundamental interpretations. Several experimental results will be presented and a special attention will be done in relation to results obtained in grain-oriented samples, which allow us to investigate anisotropic effects of the zero resistance line and the magnetic irreversibility line.

The idea that the magnetic irreversibility line is a boundary which an electric current may flow without electric resistance comes from the conventional homogeneous metallic superconductors. On the another hand, the high-temperature superconductors such as YBaCuO and other cuprates are usually granular superconductors and in this case the onset of magnetic irreversibility takes place when the first loop of coupled grains is formed. An array of coupled grains is responsible to trap the Josephson flux and establish an irreversible behavior. However in this case the electric transport remains resistive because the well-coupled grain clusters (which are responsible for the magnetic irreversibility) still remain disconnected from each other. It's important to observe that the resistivity vanishes only when the grain coupling strength overcomes the phase entropy and leads to a long-range coherence of the order parameter. As a consequence the electrical resistance in granular superconductors is expected to persist down to temperatures below the irreversibility line and to vanish only after the phase coherence percolates through the whole sample. In materials who exhibit a weak superconducting granularity the zero resistance data are expected to fall closely below the irreversibility line. Although in some cases the zero resistance line falls below the magnetic irreversibility line, some authors admitted that in high magnetic fields, where the flux dynamics is dominated by the intragrain Abrikosov flux, the zero resistance line again follows the irreversibility line. But apparently some results obtained in grain-oriented materials exclude this possibility when high magnetic fields are applied and in this case the expected behavior is not observed.

These important aspects of the correlation between magnetic irreversibility and zero resistance line will be discussed based on the main models and ideas currently accepted.

2. YBaCuO superconductor

It will be described in this section the structural properties, the main growth techniques and some potential technological applications of the YBaCuO superconductor.

2.1 Structural properties

The discovery of superconducting oxides of high critical temperature occurred in 1986 with the pioneer work by Müller and Bednorz (Müller & Bednorz, 1986), who reported the observation of the superconductivity around 30 K in a compound containing La, Ba, Cu and O. The intense interest in these systems occurred a year later, after the work of Wu et al. (Wu et al., 1987) who substituted lanthanum by yttrium in the original formula of Müller and Bednorz. The critical temperature increased to 93 K, well above the boiling point of liquid nitrogen. This material, $YBa_2Cu_3O_{7-\delta}$, or simply YBaCuO, was the responsible to inaugurate a new era in the materials research. The relative simplicity in growth of ceramic samples was crucial to mobilize several research groups around the world in a deep study for its physical properties, as well as possible technological applications.

Unlike conventional metallic superconductors, the crystal structure of the HTSC is complex. One of the most important characteristic in high-temperature superconductors is the planar anisotropy. Figure 1 shows the crystal structure of $YBa_2Cu_3O_{7-\delta}$ superconductor.

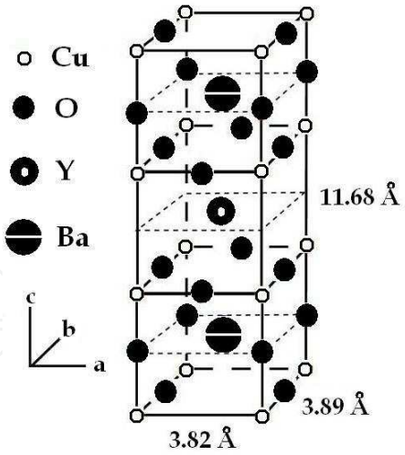

Fig. 1. The crystal structure of $YBa_2Cu_3O_{7-\delta}$ superconductor.

The typical lattice parameters are a = 3.82 Å, b = 3.89 Å and c = 11.68 Å. As shown in Figure 1, the $YBa_2Cu_3O_{7-\delta}$ superconductor is a perovskite-type cuprate with orthorhombic symmetry and the main structural characteristic is the presence of Cu-O_2 double planes separated by an yttrium atomic layer. The Cooper pairs, responsible to superconducting properties, are placed in the CuO_2 double planes. The atomic structures between the conducting planes are denominated charge reservoir. The oxygen content can vary between 6 and 7 atoms by unit cell. Deoxygenated systems ($\delta = 1$ or simply 6 oxygen atoms per unit cell) has tetragonal structure and insulating anti-ferromagnet behaviour. For the optimum oxygen content of $\delta \approx 0.07$ the $YBa_2Cu_3O_{7-\delta}$ system has the biggest superconducting temperature at around 93 K.

2.2 Growth techniques

Several techniques have been employed to grow superconducting samples of $YBa_2Cu_3O_{7-\delta}$. It's possible to prepare samples as bulk (polycrystalline sintered or melt-textured), thin films and single crystals, among others. Initially the sintering procedure was the most promising technique because of its simplicity and possibility to obtain samples in a specific desired shape. The samples obtained by sintering techniques in general present a microstructure characterized by reduced grain size (few μm), porosity, cracks or microcracks and an aleatory grain alignment. This microstructure is responsible for the low critical current density values observed in sintered samples as compared to single-crystalline samples.

The melt-textured techniques have arisen as an alternative way to produce samples with high critical current density values needed for some technological applications. The pioneer work by Jin et al. (Jin et al., 1988a) set the basis to the melt-textured growth of $YBa_2Cu_3O_{7-\delta}$ samples. Melt-textured samples exhibit a microstructure characterized by large grains, low-angle grain boundaries, directional alignment (c-axis oriented), reduced porosity and dense structure. This microstructure plays an important role at the high critical density current values observed in melt-textured samples. Figure 2 shows a comparative image of (a) sintered and (b) melt-textured $YBa_2Cu_3O_{7-\delta}$ samples (Jin et al., 1988b).

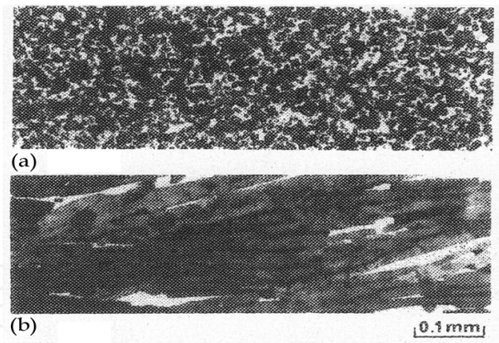

Fig. 2. Comparative image of (a) sintered and (b) melt-textured YBaCuO samples. From Jin et al.

Due to the large size of the oriented single domains obtained by melt-textured processes is possible to access directly the physics properties along the c-axis, such as electrical transport. Some works have been done using this important characteristic to study, for example, conductivity fluctuations in melt-textured $YBa_2Cu_3O_{7-\delta}$ samples (Jurelo et al., 2008; Dias et al., 2009).

$YBa_2Cu_3O_{7-\delta}$ samples can be grown as thin films and several techniques have been employed. Recently the chemical solution deposition (CSD technique) has been the more attractive technique due to its low cost and high performance of the samples obtained by this method. The growth of $YBa_2Cu_3O_{7-\delta}$ samples by metal-organic decomposition (MOD) using trifluoroacetate precursor solutions is used to produce high-performance superconductor thin films, as reviewed by some authors (Sandiumenge et al., 2006; Araki & I. Hirabayashi, 2003; Obradors et al., 2004).

2.3 Technological applications

The $YBa_2Cu_3O_{7-\delta}$ superconductor is the more used high-T_C system for technological applications due to its high critical current density and high-performance in applications involving high-magnetic fields. The relative facility in the growth of samples with specific shape permits their use in large scale. Due to the high performance in magnetic and electrical properties the materials prepared by melt-textured and thin films techniques have contributed decisively in this direction.

Several applications involving $YBa_2Cu_3O_{7-\delta}$ superconductor have been made since its discovery in 1987. Masato Murakami (Murakami, 2000) proposed two definitions for classify the applications of bulk high-temperature superconductors, named passive applications and magnet applications. In passive applications the high-temperature superconductors can be used in superconducting bearing systems, flywheels, cryogenic pumps, hysteresis motors (as rotor), etc. Examples for magnet applications include quasi-permanent magnets, maglev trains, magnetic clamps, motors (as stator), magnetic bumpers, in high-field physics, magnetization devices.

An important review by David Larbalestier et al. (Larbalestier et al., 2001) on power applications of high-T_C superconductors points out the need to low-cost fabrication associated to high-performance in electric current transport. This would allow producing

large-scale superconducting electric devices for power industry, such as power cables, magnetic energy-storage devices, transformers, fault current limiters, etc. $YBa_2Cu_3O_{7-\delta}$ superconductor is pointed as one of the best candidates for these applications.

The importance of high-performance in current transport associated with a low-cost process to the fabrication of single grain bulk superconductors is also pointed out as one of main factors to effective applications in engineering devices by Hari Babu et al. (Hari Babu et al., 2011).

3. Fundamental properties

This section is dedicated to a review about electrical and magnetic properties of the high-temperature superconductors, with special attention to the $YBa_2Cu_3O_{7-\delta}$ system.

3.1 Electrical transport properties

In this sub-section it will be discussed some fundamental aspects of the electric properties of the high-temperature superconductors, with emphasis in the anisotropy of the normal state and in the granularity and disorder effects.

3.1.1 Anisotropy of the normal state

The transport properties of the high-temperature superconductors are highly anisotropic due to their crystalline structure. The CuO_2 atomic planes (ab planes) are good conductors but separated by highly resistive sheets, resulting in a strong planar anisotropy, with a low conductivity along the c-axis. The electrical current transport in $YBa_2Cu_3O_{7-\delta}$ superconductor is metallic-type along the ab plane. The same transport behaviour along the c-axis is also achieved in good quality samples. Figure 3 shows the electrical resistivity behaviour along the three crystallographic axes for an untwinned $YBa_2Cu_3O_{7-\delta}$ single crystal. The strong anisotropic character can be observed with a ratio at room temperatures of $\rho_a/\rho_b \approx 2.5$ and $\rho_c/\rho_a \approx 30$.

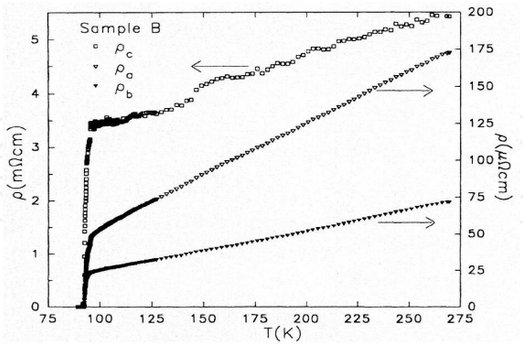

Fig. 3. Electrical resistivity behaviour along the three crystallographic axes for an untwinned $YBa_2Cu_3O_{7-\delta}$ single crystal. From Friedmann et al.

3.1.2 Granularity and disorder

The coherence length (T = 0 K) of an $YBa_2Cu_3O_{7-\delta}$ superconductor is approximately 12-20 Å along the ab plane and 1-3 Å along the c-axis, while the penetration length is about 1000 Å.

As a consequence the $YBa_2Cu_3O_{7-\delta}$ system is classified as an extreme type-II superconductor. Therefore defects of the same (or higher) order of magnitude are very important in these materials. The high-temperature superconductors present several intrinsic defects in different size scales: macroscopic (grain-boundaries, porosity, non-superconducting phases, such as the $Y_2Ba_1Cu_1O_5$ phase in some melt-textured $YBa_2Cu_3O_{7-\delta}$ samples), mesoscopic (twin-planes, dislocations, stacking-faults, columnar defects) and microscopic (oxygen vacancy, substituting atoms). The existence of these defect levels is responsible for the complex topology of the order parameter. Samples with higher disorder degree present an intrinsic and complex granularity, and this inhomogeneous character reflects in the magnetic and transport properties. Disorder is relevant since discovery of the HTSC's, when its presence was associated to the superconducting-glass state (Ebner & Stroud, 1985).

The resistive transition to the superconducting state in granular systems occurs in two steps-like transition, defining two important temperatures, namely T_C and T_{C0}, as presented in Figure 4.

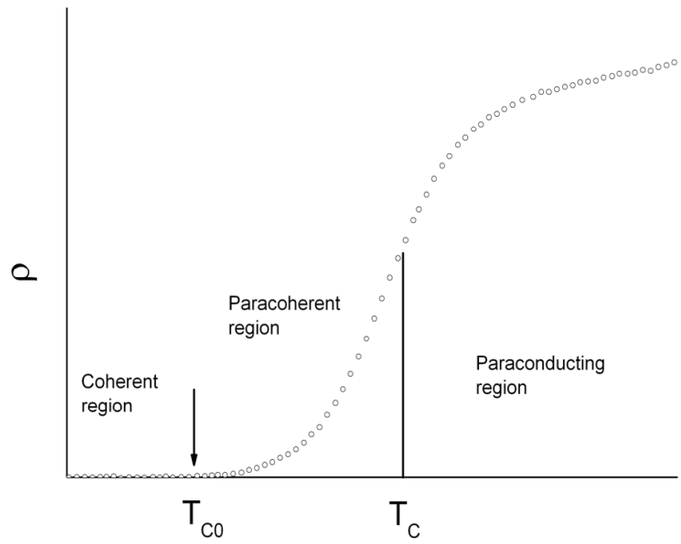

Fig. 4. Resistive transition in a granular superconductor.

The region above T_C is called "paraconducting" region and the excess of conductivity is attributed to thermal fluctuations of the amplitude of the order parameter. T_C is practically coincident with the bulk critical temperature, and the superconductivity stabilizes in homogeneous and mesoscopic regions of the sample (grains). Between T_C and T_{C0} the superconducting grains are weakly coupled to each other by Josephson effect and thermal fluctuations occur in the phase of the order parameter of the grains. This region is called "paracoherent" region and the electrical resistivity is not zero. The long-range superconducting state is achieved at T_{C0} through a percolation process at the grains. This process controls the activation of weak links between the superconducting grains and is called coherence transition. A detailed investigation of this process is given by Rosenblatt et al. (Rosenblatt et al., 1988). At the critical temperature (T_{C0}) where the coherence transition sets in, the fluctuating phases of the order parameter in each grain couple to each other into a long-range ordered state and a zero resistivity state is established.

3.2 Magnetic properties

In this section it will be discussed some fundamental aspects of the magnetic properties of the high-temperature superconductors, focusing in the irreversibility behaviour of the magnetization.

3.2.1 Phase diagram

The zero resistivity and the perfect diamagnetism (Meissner effect) are the main characteristics to any material be considered a superconductor. The Figure 5 shows a mean-field type phase diagram for a type-II superconductor, such as $YBa_2Cu_3O_{7-\delta}$. Type-II superconductors present a perfect diamagnetism (Meissner effect) just when the applied magnetic field is lower than $H_{C1}(T)$, called as lower critical field. Consequently this region is known as Meissner state. For applied magnetic fields in the region between $H_{C1}(T)$ and $H_{C2}(T)$, the magnetic flux can penetrate inside the superconductor in form of filamentary structures known as vortices. This state is titled as mixed state and the $H_{C1}(T)$ value marks the penetration of the first magnetic flux-line inside the superconductor. When the external magnetic field is higher than $H_{C2}(T)$ (also known as upper critical field), the superconductivity is suppressed and the material passes to the normal state.

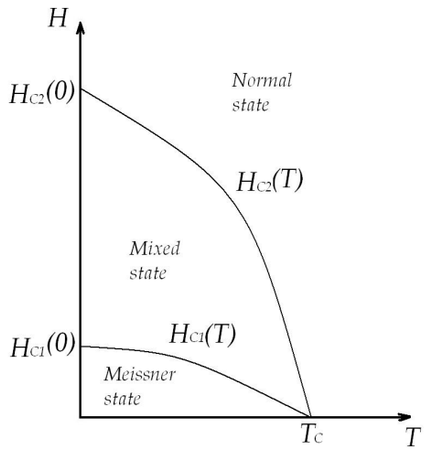

Fig. 5. Mean-field type phase diagram for a type-II superconductor.

3.2.2 Mixed state and vortex structure

The Figure 6 shows the mixed state structure in a superconducting sample where H_a is the applied magnetic field ($H_a > H_{C1}$). The Figure 6(a) shows a lattice of normal cores and the respective associated vortices, while the Figure 6(b) shows the variation with position of superparticles density (superelectrons density or Cooper pairs density).

The Figure 6(c) shows the variation of flux density with position. The superparticles density, designed by n_S, falls to zero at the centre of each isolated vortex, and the dip in the n_S is about two coherence lengths wide. The flux density in not cancelled inside the normal cores, but decreases into a small value in a distance about λ (London penetration length) away from the normal cores, as shown in Figure 6(c). Each individual vortex is surrounding by the shielding currents and the total flux generated is just one fluxon Φ_0, given by 2.067×10^{-15} Weber.

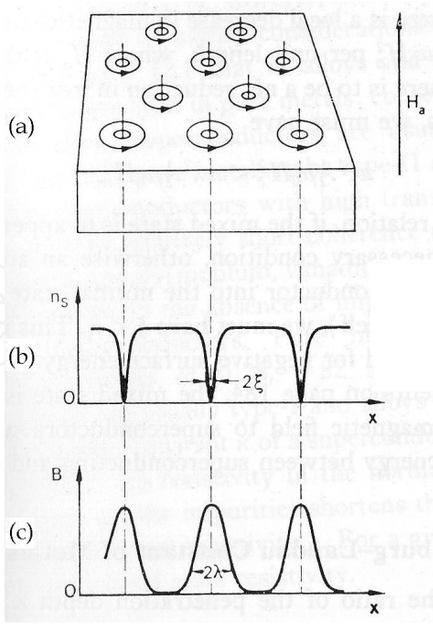

Fig. 6. The mixed state structure in a type-II superconductor. The Figure (a) shows a lattice of normal cores and the respective vortices, while the Figure (b) shows the variation with position of superparticles density and the Figure (c) shows the variation of flux density with position. From Rose-Innes & Rhoderick.

The interaction between vortices is repulsive and mediated by the Lorenz force. In a homogeneous superconductor the cores are arranged in a hexagonal (triangular) periodic array due to lower energy state. This array is known as Abrikosov lattice and can be observed in the Figure 6(a). In granular superconductors the vortices placed inside the superconducting grains are denominated intragranular vortices and are arranged in this lattice type.

The vortices can be pinned by defects of the crystal lattice. This effect is known as flux pinning and the mechanism can be improved by introducing microstructural or compositional changes like irradiation, chemical doping or precipitates.

In an isotropic and perfect superconductor (without the presence of defects) the vortices can be arranged in an Abrikosov lattice (hexagonal lattice). In a granular material, the superconducting grains can be coupled by Josephson effect, and based on this idea John R. Clem proposed a theoretical model to describe a granular superconductor using the Josephson effect as starting point (Clem, 1988). In this model a granular superconductor can be represented as anisotropic grains coupled by Josephson junctions (junctions based on Josephson effect).

The magnetic field can penetrate into a granular superconductor in the region between the grains, in the form of intergranular vortices, known as Josephson vortices. An intergranular Josephson vortex transports just one fluxon, similar to intragranular Abrikosov vortex and the magnetic structures are similar. The main difference is the region where both vortices are located. The Figure 7 shows a scheme of both vortices in a superconducting granular sample.

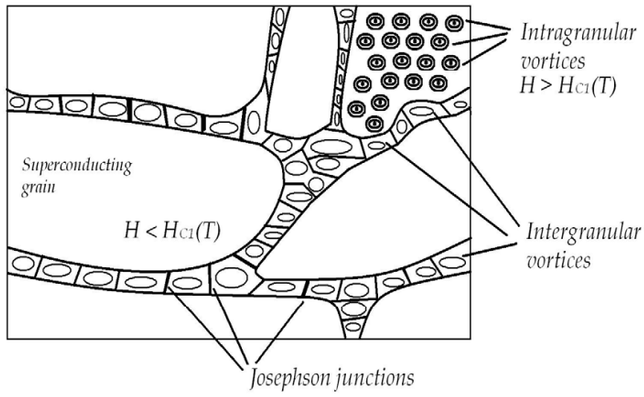

Fig. 7. Representative scheme showing intragranular and intergranular vortices in a type-II superconductor.

3.2.3 Magnetic irreversibilities

The magnetization of high-T_C superconductors shows an irreversible behaviour due to flux pinning combined with thermal activation of the vortices. In the next sections will be discussed the origin, the characteristics and some theoretical models used to explain this behaviour.

3.2.3.1 Magnetic irreversibility line

Through the realization of experiments based on ZFC (zero-field cooling) and FC (field-cooling) procedures in a superconducting sample it's possible to observe strong magnetic irreversibility effects, such as presented by Figure 8, due to flux pinning into the sample.

Below a temperature called irreversibility temperature (T_{irr}), the ZFC and FC curves present distinct behaviours. Below T_{irr} the vortices have its mobility strongly decreased due to pinning centres. As T_{irr} is dependent on the magnetic applied field, it´s possible to obtain a H versus T phase diagram similar to the one presented in Figure 9, where the line separate the diagram in two distinct regions: a region of high temperatures ($T > T_{irr}$) where the magnetization is reversible, and a region of low temperatures ($T < T_{irr}$) where the magnetization is irreversible. This line is known as magnetic irreversibility line or simply irreversibility line (IL). The study of the irreversibility line was originated with the pioneer work by Müller et al. in granular samples of $La_{2-x}Ba_xCuO_{4-\delta}$ superconductor (Müller et al., 1987).

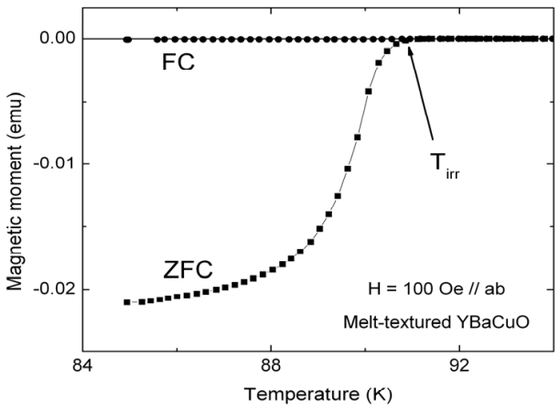

Fig. 8. Magnetic irreversibility effects in a superconducting sample obtained through the realization of ZFC (zero-field cooling) and FC (field-cooling) procedures.

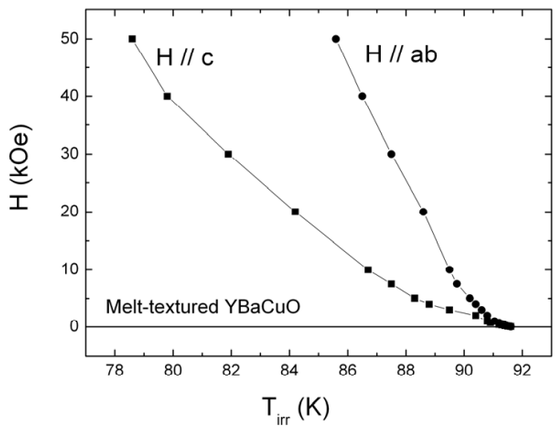

Fig. 9. The anisotropic character of the magnetic irreversibility line in a melt-textured sample.

The Figure 9 shows the anisotropic character of the magnetic irreversibility, attributed to intrinsic planar structure of the high-temperature superconductors. When H // ab the intrinsic pinning mechanism is evidenced and the vortices have their mobility restricted to the ab plane, reinforcing the effective pinning. By another hand, when H // c the lattice take the form of a stacked two-dimensional pancake-type vortices confined to the ab planes weakly coupled. At low temperatures the vortex lattice can be stabilized in a three-dimensional arrangement, but at high temperatures the thermal depinning effects passes to be relevant and a crossover from 3D to 2D occurs, resulting in a two-dimensional lattice of pancake vortices (Vinokur et al., 1990).

3.2.3.2 Theoretical models

This section is dedicated to describe some of the main models used to explain the magnetic irreversibility line (IL).

3.2.3.2.1 Giant flux creep

The model was proposed by Yeshurun and Malozemoff (Yeshurun & Malozemoff, 1988) based on the flux creep model initially developed by Anderson and Kim (Anderson & Kim, 1964). This model is based on the thermal activation effects of the vortex lattice. The model assumes that a vortex can be thermally activated over a pinning barrier even if the Lorentz force exceeds the pinning force. The main differences between both models are the high temperature and the low energy of the vortex pinning presented by the high-temperature superconductors.

According to the authors the experimental behaviour presented by the IL in a H versus T diagram obeys the power-law

$$H^{2/3} \propto (1-t) \quad , \tag{1}$$

where $t = T_{irr}/T_C$ is the reduced temperature and T_{irr} is the irreversibility temperature.

According to the giant flux creep model the IL is essentially a depinning line in a H versus T phase diagram. Above the IL the vortices can move freely resulting in a zero critical current density while below the IL a finite value occurs once the vortices are pinned.

3.2.3.2.2 Vortex melting

According to this model the thermal fluctuations are responsible by the melting of the Abrikosov lattice, and the IL behaves as a boundary between two regions, namely vortex solid and vortex liquid. The instability produced by thermal fluctuations results in a second order phase transition of the vortex lattice at a temperature called vortex lattice melting temperature, or T_M. The aleatory dislocations produced by instabilities can promote collisions and loss of correlations between vortices. According to Nelson and Seung (Nelson & Seung, 1989), when the lattice melts two new regimes can arise, namely disentangled flux liquid and entangled flux liquid. The criterion used to define the vortex melting is known as Lindemann criterion (Lindemann, 1910).

The Figure 10 shows a representation of the vortex lattice melting phases. The disentangled flux liquid is characterized by high temperatures and low flux-line densities, as represented in Figure 10(b). The entangled flux liquid is reached when the flux-line density is high, as presented in Fig. 10(c). According to Houghton et al. (Houghton et al., 1989) the melting temperature (T_M) is slightly lower than the critical temperature (T_C) and the behaviour follow the power law

$$(1-t)^2 \approx H \, , \tag{2}$$

where $t = T/T_C$ is the reduced temperature.

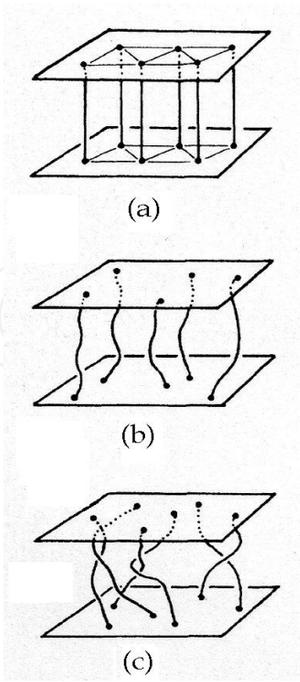

Fig. 10. Representation of the vortex lattice melting phases, showing (a) the Abrikosov lattice, (b) the disentangled and (c) the entangled flux liquid. From Nelson & Seung.

The Figure 11 shows experimental results obtained in an untwinned single crystal of $YBa_2Cu_3O_{7-\delta}$. The solid curve represents a fitting using equation (2).

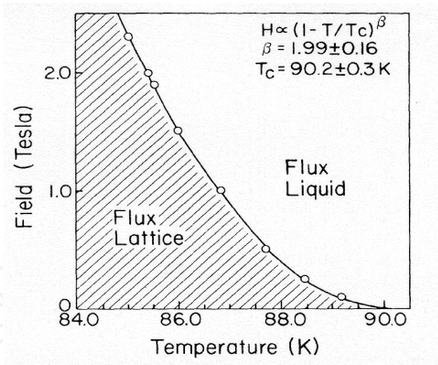

Fig. 11. H versus T phase diagram for the flux melting regime obtained in an untwinned single crystal of $YBa_2Cu_3O_{7-\delta}$. The solid curve represents a fitting using equation (2). From Farrell et al.

3.2.3.2.3 Superconducting glass

This model was based on the propositions of Ebner and Stroud (Ebner & Stroud, 1985) to study the diamagnetic susceptibility of superconducting clusters. The superconducting glass model proposes the existence of a disordered array of superconducting grains weakly coupled by Josephson effect or proximity effect. The Hamiltonian used to describe a system of weakly coupled grains is given by

$$H = -\sum_{i,j} J_{ij}\cos(\theta_i - \theta_j - A_{ij}) , \tag{3}$$

where J_{ij} is the phase coupling energies between neighboring grains i and j and θ_i - θ_j is the phase difference of the Ginzburg-Landau parameter on the grains i and j. The phase displacements A_{ij}, caused by the applied magnetic field, are given by

$$A_{ij} = \frac{2\pi}{\varphi_0}\int_i^j \vec{A}.d\vec{l} , \tag{4}$$

where ϕ_0 is the elementary flux quantum (fluxon), and the line integral is evaluated between the centres of grains i and j.

This model predicts the existence of a low temperature phase called superconducting glass, where disorder and frustration are dominants. The irreversibility line (IL) can be interpreted as a separation between two phases: namely superconducting glass and a system of decoupled grains. According to Müller et al. (Müller et al., 1987) it's possible to correlate the functionality of the IL with the same functionality used in spin glass systems. Using this analogy Müller et al. proposed that the behaviour of the IL at low applied magnetic fields in high-T_C superconductors can be described by de Almeida-Thouless type power law (de Almeida & Thouless, 1978), and it's given by

$$H = H_0\left(1 - \frac{T_g(H)}{T_g(0)}\right)^{\gamma} , \tag{5}$$

where $\gamma = 3/2$ and $T_g(H)$ can be interpret as $T_{irr}(H)$ in superconducting materials. The Figure 12 shows experimental results obtained in a $La_2BaCuO_{4-\delta}$ sample. The solid curve represents a numerical fit using equation (5). Another similarity occurs when higher magnetic fields are applied. In this case it's possible to observe a crossover from de Almeida-Thouless to Gabay-Toulouse (Gabay & Toulouse, 1981), where the behaviour can be described by the power law

$$H = \beta\left(1 - \frac{T_{irr}(H)}{T_{irr}(0)}\right)^{1/2} , \tag{6}$$

where β is a constant and $T_{irr}(H)$ and $T_{irr}(0)$ are the irreversibility temperatures obtained when $H \neq 0$ and $H = 0$.

3.2.3.2.4 Vortex glass

The vortex glass model was proposed by Fisher (Fisher, 1989) to describe the crossover from reversible to irreversible magnetization in high-T_C superconducting oxides using disorder effects. This model predicts the existence of a vortex glass phase between the Meissner state and the line defined by the temperature $T_G(H)$, as showed in Figure 13. The Abrikosov lattice in the vortex glass state has no long-range symmetry and the vortices freeze in a 2D lattice exhibiting a low-range order. The disorder and frustration are related to aleatory pinning centres distribution. As the temperature increases the vortex glass can be

destabilized by thermal fluctuations and it melts above the $T_G(H)$ line, defining a state known as vortex liquid, as showed in Figure 13. The $T_G(H)$ line can be identified as the irreversibility line (IL).

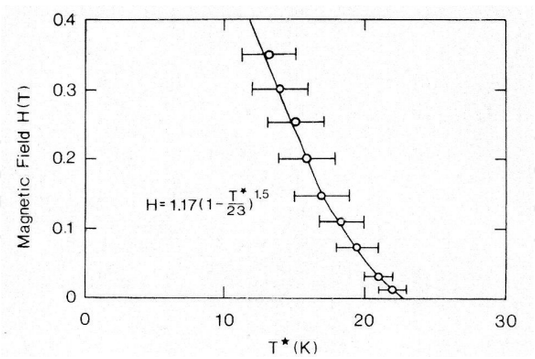

Fig. 12. Irreversibility line obtained in a $La_2BaCuO_{4-\delta}$ sample. The solid curve represents a numerical fit using equation (5). From Müller et al.

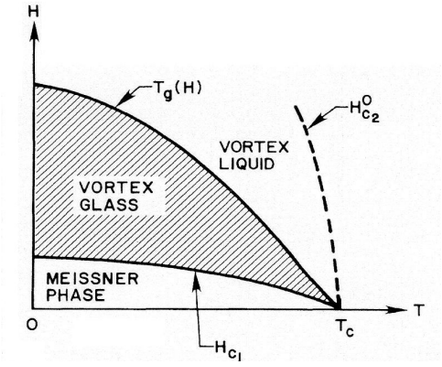

Fig. 13. Phase diagram for the vortex glass model. The $T_G(H)$ line can be identified as the irreversibility line (IL). From Fisher.

3.2.3.2.5 Bose glass

The Bose glass theory was developed by Nelson and Vinokur (Nelson & Vinokur, 1992) to treat the effects due to flux pinning by correlated defects (columnar defects, twin planes, grain boundaries, etc.). For a high-temperature superconductor with strongly correlated disorder the model predicts a H versus T diagram divided into three phases: superfluid, Bose glass and Mott insulator.

The superfluid phase is characterized by high temperature and viscous motion of vortices, which can jump across the correlated defects trough the sample. The Bose glass phase is essentially characterized by the strongly anisotropic pinning due to extended and correlated defects in the sample. This behaviour is strongly dependent on the alignment between the applied magnetic field and the direction of the defects dispersed in the superconducting sample. Misalignments greater than 5° may remove this phase in accordance with experimental results obtained by Safar et al. (Safar et al., 1996) in twinned $YBa_2Cu_3O_{7-\delta}$ single crystals. The Mott insulator phase occurs at low temperatures and can be characterized by a highly non-linear vortex dynamics governed by similar properties to the Meissner state.

4. Correlations between the magnetic irreversibility and the resistive transition

This section will be dedicated to present and to discuss experimental results on the magnetic irreversibility line, on the zero resistance line and on the respective correlations in high-temperature superconductors. The results will be focused in the $YBa_2Cu_3O_{7-\delta}$ superconductor.

4.1 Brief considerations

The magnetic irreversibility line in homogeneous superconductors defines a boundary in the H versus T plane below which the magnetization is irreversible and up to which a nonzero electric current can flow without any electrical resistance. Above this line the magnetization is reversible and all electric transport is resistive due to dissipation by flux dynamic effects. Very clean and well-oxygenated $YBa_2Cu_3O_{7-\delta}$ single crystals can be considered homogeneous superconductors and in this case the electrical resistivity is expected to vanish at the irreversibility line and even to comply with the planar anisotropy of the magnetic irreversibility. However high-temperature superconducting cuprates are generally inhomogeneous superconductors (Vieira & Schaf, 2002) or intrinsically inhomogeneous (Dagotto, 2005).

The magnetic irreversibility and the electrical resistivity in granular superconductors do not depend on the same parts of the superconducting sample. While the irreversibility depends on well-coupled grain clusters, the electrical resistance depends on grain arrays traversing the whole sample. Along such long-range paths, zero electrical resistance can be attained only at some temperature below the irreversibility temperature (Rosenblatt et al., 1988). On the other hand, at magnetic fields above several kOe the magnetic field penetrates the grains and the magnetic irreversibility is dominated by the Abrikosov flux dynamics (intragrain flux) while the electrical resistivity is still ruled by the grain junctions and can vanish only after the achievement of a long-range coherence state.

Magnetic irreversibility studies on pure and doped $YBa_2Cu_3O_{7-\delta}$ single crystals (Schaf et al., 2001, 2002) show the signature of superconducting granularity in the low-field region, dominated by Josephson flux (intergrain flux). Although in some cases the data for zero resistance falls below the magnetic irreversibility line, the authors admitted that in high magnetic fields, where the flux dynamics is dominated by the Abrikosov flux, the zero resistance line again follows the irreversibility line (Pureur et al., 2000, 2001).

High-quality melt-textured $YBa_2Cu_3O_{7-\delta}$ materials normally do not exhibit the signature of superconducting granularity, in spite of the polycrystalline structure. The linking between the crystallites is so strong that in some cases the coupling between superconducting grains occurs almost simultaneously with the superconducting transition.

4.2 Experimental results in YBaCuO superconductors

The results in this section are presented for several $YBa_2Cu_3O_{7-\delta}$ samples grown by different techniques, and some of experimental results and discussions were previously published by Schaf et al. (Schaf et al., 2008) and Dias et al. (Dias et al., 2008).

The Figure 14 shows results in an $YBa_2Cu_{2.97}Zn_{0.03}O_{7-\delta}$ single crystal grown by self-flux method. The continuous lines represent the irreversibility lines, $T_{irr}(H)$, for H // ab and

H // c and are fits to the power law predicted by the giant-flux-creep theory, while the circles represent the zero resistance data, $T_{C0}(H)$, for H // ab and H // c. The inset in the Figure 14 highlights the data at low magnetic fields where the continuous lines are fits to the de Almeida-Thouless and Gabay-Toulouse power laws. The $T_{irr}(H)$ data show a weak superconducting granularity and consequently the zero resistance data are expected to fall closely below the irreversibility line, as showed in the Figure 14. While at high magnetic fields the $T_{C0}(H)$ data fall about the irreversibility lines, in the low-field region they fall systematically underneath the irreversibility line for both field configurations (see inset).

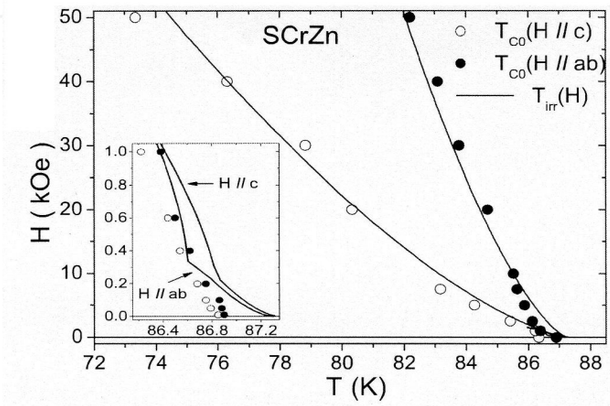

Fig. 14. Irreversibility lines in an $YBa_2Cu_{2.97}Zn_{0.03}O_{7-\delta}$ single crystal, together with the zero resistance data T_{C0}. The closed circles are for fields applied parallel to the ab plane and the open circles are for fields along the c-axis. The inset highlights the data in low fields. From Schaf et al.

The data in the Figure 15 illustrates the case of a melt-textured $YBa_2Cu_3O_{7-\delta}$ sample grown by top-seeding technique and containing 30 wt% of Y_2BaCuO_5 (Y211 phase) and 1 wt% of CeO_2. The purpose of the Y211 phase is to introduce pinning centers and the CeO_2 physically stabilizes the melt at high temperatures during the growth, to limit the size of the Y211 particles and to improve the distribution of the Y211 phase. This procedure strongly enhances the flux pinning potential in melt-textured $YBa_2Cu_3O_{7-\delta}$ samples. On the other hand, high-quality melt-textured samples in general do not display superconducting granularity. However, the high concentration of Y211 phase causes considerable misalignment of the c-axis, thereby encumbers the grain coupling and reduces the planar anisotropy (Carrillo et al., 2000). The weak superconducting granularity presented by the melt-textured sample, whose results are presented in the Figure 15, arises mainly from misalignment of the c-axis, resulting in a reduced planar anisotropy.

In the Figure 15 the irreversibility lines (H // ab and H // c) are represented by the experimental data and the continuous lines are fits to the power law predicted by the giant-flux-creep theory. The measuring current in the zero resistance data flows along the same ab planes for both field orientations (H // ab and H // c). While for H // ab plane and H // J the zero resistance data (closed circles) fall closely underneath the corresponding irreversibility line, they split strongly away from the irreversibility line toward lower temperatures for H // c and H ⊥ J (open circles).

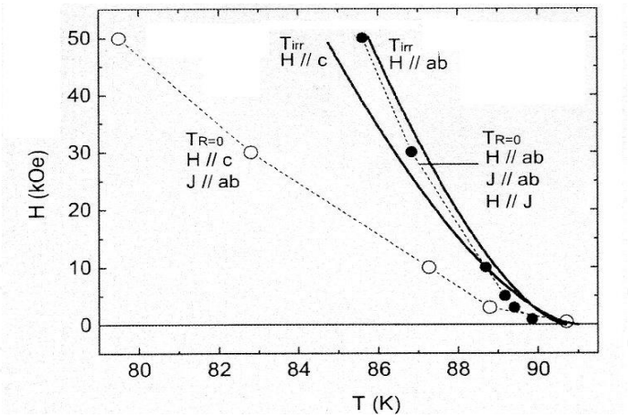

Fig. 15. Irreversibility lines obtained in a melt-textured $YBa_2Cu_3O_{7-\delta}$, together with the zero resistance data T_{C0}. The closed circles are for fields applied parallel to the ab plane and the open circles are for fields along the c-axis. From Schaf et al.

The twinning domains in the investigated melt-textured sample are nearly random in the ab plane and their direction also must be scattered somewhat about the average c-axis, due to the misalignment of the c-axis. Therefore, while flux pinning by the twinning planes certainly contributes somewhat for fields applied along the c-axis, its contribution for fields along the ab plane must be irrelevant. In the Figure 15 the irreversibility data show a much reduced anisotropy, due to the spreading out of the c-axes of the different crystallites and the consequent noncoplanarity of the ab planes.

Similar results (not published) are showed in the Figure 16, for a $YBa_2Cu_3O_{7-\delta}$ thin film grown by chemical solution deposition. It can be observed that the zero resistance data for H // c and H $\perp$ J split away from the irreversibility line (H // ab) towards lower temperatures.

The data in the Figure 17 are representative for a polycrystalline $YBa_{1.75}Sr_{0.25}Cu_3O_{7-\delta}$ sample grown by conventional sintered technique using the standard solid state reaction method (Schaf et al., 2008). This polycrystalline sample exhibits a strong superconducting granularity, as shown by the presence of the de Almeida-Thouless and Gabay-Toulouse regimes in the low-field irreversibility data. The asterisks in the Figure 17 denote the approximate superconducting temperature transition (T_C); the open circles are the irreversibility data; the closed circles are the zero resistance data (T_{C0}) and the continuous lines are fits to de Almeida-Thouless, Gabay-Toulouse and giant-flux creep power laws.

In spite of the magnetic field being applied parallel to the measuring current, H // J, the zero resistance data of this polycrystalline sample fall considerably below the irreversibility line already in low magnetic fields and split away from this line steeply when the applied magnetic field increases. In polycrystalline samples the current flow through the grain aggregate is highly dispersive and therefore the H // J configuration is only a microscopic approximation. The data in the Figure 17 also show no indication the zero resistance data might come back and meet the irreversibility line somewhere in higher magnetic fields.

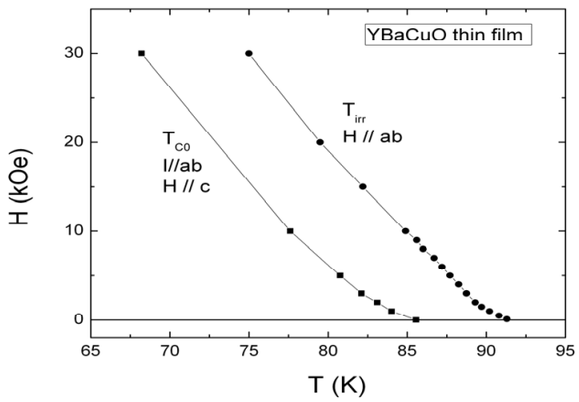

Fig. 16. Irreversibility line (T_{irr}) and zero resistance data (T_{C0}) obtained in a $YBa_2Cu_3O_{7-\delta}$ thin film. The closed circles are for fields applied parallel to the ab plane and the closed squares are for fields along the c-axis. Not published.

An applied magnetic field to a granular superconductor increases the phase entropy (Stroud et al., 1984). This magnetic field, while randomly produces a distortion of the phase of the order parameter, weakens and frustrates the grain coupling and favors the phase fluctuations that can result in the increase of the magnetoresistance. The random phase distortions also weakens the ability of the grain aggregate to pin the intergrain Josephson flux that dominates in the low-field regime. Therefore, in the low-field regime the irreversibility line exhibits the de Almeida-Thouless and Gabay-Toulouse power laws that are the signature of frustrated systems.

The response of a granular superconductor to a magnetic field is usually described in terms of the Josephson coupling Hamiltonian given by the equation (3) together with the equation (4). The equation (4) shows that a magnetic field causes phase displacements of the Ginzburg-Landau order parameter along those weak links which extend along the vector potential A , i.e. the A_{ij} are large along weak links that lie transversely to the magnetic field but may vanish along the weak links oriented parallel to the magnetic field.

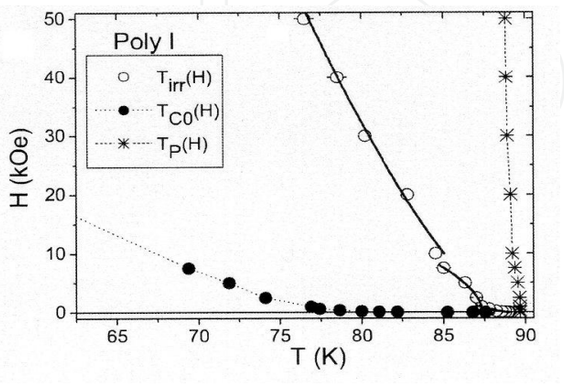

Fig. 17. Irreversibility line (T_{irr}) and zero resistance data (T_{C0}) in a polycrystalline $YBa_{1.75}Sr_{0.25}Cu_3O_{7-\delta}$ sample. The asterisks indicate the approximate superconducting transition temperatures. From Schaf et al.

Due to the dependence of the phase displacements A_{ij} and the associated grain decoupling effect on the direction of the applied field with respect to the weak links, the magnetic irreversibility line and the zero resistance of granular superconductors depend strongly on the field-current configuration. For instance, if the magnetic field is applied along the c-axis and the current flows in the ab plane, the degradation of the conducting junctions is expected to be strong and leads to a considerable increase of the resistivity and a large displacement of the zero resistance temperature towards lower temperatures. A representative result can be observed in the Figure 15. On the other hand, if the magnetic field orientation is parallel to the current in the ab plane, the effect of the field on the weak links carrying the current is expected to be much smaller, and this can be seen also in the Figure 15.

In the case of the polycrystalline sintered sample, in which the links between the grains are much weaker, the effects of the applied field on the grain coupling is drastic even for fields applied parallel to the intended measuring current, as can be seen in the Figure 17. In these granular superconductors the direction of the current is disperse due to the coupled grain arrays that percolate through the whole sample in randomic loops.

5. Conclusion

The connection between the magnetic irreversibility limit and the zero resistance in high-T_C superconductors is very important in order to understand the mechanisms of the electric current transport in these systems. In granular superconductors the zero resistance state is ruled by grain couplings and the effect of an applied magnetic field on the electrical resistivity depends strongly on the field-current configuration. In a superconducting sample which has a weak superconducting granularity, the electrical resistance vanishes very close to and underneath the magnetic irreversibility limit. On the other hand, for samples with a strong superconducting granularity, the magnetic field severely degrades the grain couplings. The electrical resistance, for current flowing along the weak links affected by the magnetic field, vanishes far below the irreversibility line.

Because of the potential for technological applications, the correlation between electric and magnetic properties in HTSC systems can provide important information on the performance of these materials when magnetic fields are applied in different configurations.

6. Acknowledgment

I'm very grateful to Dr. Frederik Wolff-Fabris for a careful reading of the text and to Dr. Jacob Schaf, Dr. Paulo Pureur and Dr. Valdemar Vieira for important discussions. This work was partially supported by the Brazilian Ministry of Science and Technology and the State of Rio Grande do Sul, under the Grant PRONEX FAPERGS/CNPq 10/0009-2, and Ministry of Science and Technology, under the Grant CAPES/Procad 059/2007.

7. References

Almeida, J., & Thouless, D. (1978). Stability of the Scherrington-Kirkpatrick solution of a spin glass model. *Journal of Physics A,* Vol.11, No.5, (May 1978), pp. 983-990, ISSN 1751-8113

Anderson, P., & Kim, Y. (1964). Hard superconductivity: theory of the motion of Abrikosov flux lines. *Review of Modern Physics,* Vol.36, No.1, (January 1964), pp. 39-43, ISSN 0034-6861

Araki, T., & Hirabayashi, I. (2003). Review of a chemical approach to $YBa_2Cu_3O_{7-x}$-coated superconductors – metalorganic deposition using trifluoroacetates. *Superconductor Science & Technology,* Vol.16, No.11, (September 2003), pp. R71-R94, ISSN 0953-2048

Bednorz, J., & Müller, K. (1986). Possible high Tc superconductivity in the Ba-La-Cu-O system. *Zeitschrift für Physik B,* Vol. 64, No. 2, (September 1986), pp. 189-193, 0722-3277

Carrillo, A., Puig, T., Plain, J., Figueras, J., & Obradors, X. (2000). Y_2BaCuO_5-free melt textured $YBa_2Cu_3O_7$: a search for the reference sample. *Physica C,* Vol.336, No.3-4, (July 2000), pp. 213-226, ISSN 0921-4534

Chu, C., Wu, M., Ashburn, J., Torng, C., Hor, P., Meng, R., Gao, L., Huang, Z., & Wang, Y. (1987). Superconductivity at 93 K in a new mixed-phase Y-Ba-Cu-O compound system at ambient pressure. *Physical Review Letters,* Vol.58, No.9, (March 1987), pp. 908-910, ISSN 0031-9007

Clem, J. (1988). Granular and superconducting-glass properties of the high-temperature superconductors. *Physica C,* Vol.153-155, No.1, (June 1988), pp. 50-55, ISSN 0921-4534

Dagotto, E. (2005). Complexity in Strongly Correlated Electronic Systems. *Science*, Vol.309, No.5732, (July 2005), pp. 257-262, ISSN 0036-8075

Dias, F., Vieira, V., Rodrigues Jr., P., Obradors, X., Pimentel Jr., J., Pureur, P., & Schaf, J. (2008). Magnetic irreversibility and zero resistance in melt-textured YBaCuO. *Journal of Magnetism and Magnetic Materials,* Vol.320, No.14, (July 2008), pp. e481-e483, ISSN 0304-8853

Dias, F., Vieira, V., Pureur, P., Rodrigues Jr., P., & Obradors, X. (2009). Fluctuation conductivity along the c-axis and parallel to the ab-planes in melt-textured $YBa_2Cu_3O_{7-\delta}$ samples doped with Y211 phase. *Physica B,* Vol.404, No.19, (October 2009), pp. 3106-3108, ISSN 0921-4526

Ebner, C., & Stroud, D. (1985). Diamagnetic susceptibility of superconducting clusters: spin-glass behavior. *Physical Review B,* Vol.31, No.1, (January 1985), pp. 165-171, ISSN 1098-0121

Farrell, D., Rice, J., & Ginsberg, D. (1991). Experimental evidence for flux-lattice melting. *Physical Review Letters,* Vol.67, No.9, (August 1991), pp. 1165-1168, ISSN 0031-9007

Fisher, M. (1989). Vortex-glass superconductivity: a possible new phase in bulk high-T_c oxides. *Physical Review Letters,* Vol.62, No.12, (March 1989), pp. 1415-1418, ISSN 0031-9007

Friedmann, T., Rabin, M., Giapintzakis, J., Rice, J., & Ginsberg, D. (1990). Direct measurement of the anisotropy of the resistivity in the a-b plane of twin-free, single-crystal, superconducting $YBa_2Cu_3O_{7-\delta}$. *Physical Review B,* Vol.42, No.10, (October 1990), pp. 6217-6221, ISSN 1098-0121

Gabay, M., & Toulouse, G. (1981). Coexistence of spin-glass and ferromagnetic orderings. *Physical Review Letters,* Vol.47, No.3, (July 1981), pp. 201-204, ISSN 0031-9007

Hari Babu, N., Shi, Y., Pathak, S., Dennis, A., & Cardwell, D. (2011). Developments in the processing of bulk (RE)BCO superconductors. *Physica C,* Vol.471, No.5-6, (December 2010), pp. 169-178, ISSN 0921-4534

Houghton, R., Pelcovits, R., & Sudbo, A. (1989). Flux lattice melting in high-Tc superconductors. *Physical Review B,* Vol.40, No.10, (October 1989), pp. 6763-6770, ISSN 1098-0121

Jin, S., Tiefel, T., Sherwood, R., van Dover, R., Davis, M., Kammlott, G., & Fastnacht, R. (1988a). Melt-textured growth of polycrystalline $YBa_2Cu_3O_{7-\delta}$™ with high transport JC at 77K. *Physical Review B,* Vol.37, No.13, (May 1988), pp. 7850-7853, ISSN 1098-0121

Jin, S., Tiefel, T., Sherwood, R., van Dover, R., Davis, M., Kammlott, G., Fastnacht, R., & Keith. H. (1988b). High critical currents in Y-Ba-Cu-O superconductors. *Applied Physics Letters,* Vol.52, No.24, (June 1988), pp. 2074-2076, ISSN 1077-3118

Jurelo, A., Rodrigues Jr., P., de Azambuja, P., Dias, F., & Costa, R. (2008). Fluctuation conductivity in melt-textured $YBa_2Cu_3O_{7-\delta}$. *Modern Physics Letters B,* Vol.22, No.18, (March 2008), pp. 1717-1725, ISSN 0217-9849

Larbalestier, D. Gurevich, A., Feldmann, D. & Polyanskii, A. (2001). High-T_C superconducting materials for electric power applications. *Nature,* Vol.414, (November 2001), pp. 368-377, ISSN 0028-0836

Lindemann, F. (1989). The calculation of molecular vibration frequencies. *Physik Zeitschrift,* Vol.11, No.14, (July 1910), pp. 609-612

Müller, K., Takashige, M., & Bednorz, J. (1987). Flux trapping and superconductive glass state in La_2CuO_{4-y}:Ba. *Physical Review Letters,* Vol.58, No.11, (March 1987), pp. 1143-1146, ISSN 0031-9007

Murakami, M. (2000). Progress in applications of bulk high temperature superconductors. *Superconductor Science & Technology,* Vol.13, No.5, (May 2000), pp. 448-450, ISSN 0953-2048

Nelson, D., & Seung, H. (1989). Theory of melted flux liquids. *Physical Review B,* Vol.39, No.13, (May 1989), pp. 9153-9174, ISSN 1098-0121

Nelson, D., & Vinokur, V. (1992). Boson localization and pinning correlated disorder in high-temperature superconductors. *Physical Review Letters,* Vol.68, No.15, (April 1992), pp. 2398-2401, ISSN 0031-9007

Obradors, X., Puig, T., Pomar, A., Sandiumenge, F., Piñol, S., Mestres, N., Castaño, O., Coll, M., Cavallaro, A., Palau, A., Gázquez, J., González, J., Gutiérrez, J., Romà, N., Ricart, S., Moretó, J., Rossell, M., & van Tendeloo, G. (2004) Chemical solution deposition: a path towards low cost coated conductors. *Superconductor Science & Technology,* Vol.17, No.8, (June 2004), pp. 1055-1064, ISSN 0953-2048

Pureur, P., Costa, R., Roa-Rojas, J., & Prieto, P. (2000). Pairing transition, coherence transition, and the irreversibility line in granular $GdBa_2Cu_3O_{7-\delta}$. *Physical Review B,* Vol.61, No.18, (May 2000), pp. 12457-12462, ISSN 1098-0121

Pureur, P., Roa-Rojas, J., & Fabris, F. (2001). Magnetotransport properties and the irreversibility line in ceramic $DyBa_2Cu_3O_{7-\delta}$. *Physica C,* Vol.354, No.1-4, (May 2001), pp. 304-308, ISSN 0921-4534

Rose-Innes, A., & Rhoderick, E. (1994). *Introduction to Superconductivity* (Revised second edition). Pergamon, ISSN 0-08-021652-8, Great Britain

Rosenblatt, J., Peyral, P., Raboutou, A., & Lebeau, C. (1988). Coherence in 3D networks: Application to high-T_c superconductors. *Physica B,* Vol.152, No.1-2, (August 1988), pp. 95-99, ISSN 0921-4526

Safar, H., Foltyn, S., Jia, Q., & Maley, M. (1996). Bose glass vortex phase transition in twinned $YBa_2Cu_3O_{7-\delta}$ superconductors. *Philosophical Magazine B,* Vol.74, No.5, (November 1996), pp. 647-654, ISSN 1364-2812

Sandiumenge, F., Gázquez, J., Coll, M., Pomar, A., Mestres, N., Puig, T., Obradors, X., Kihn, Y., Casanove, M., & Ballesteros, C. (2009). Precursor Evolution and Nucleation Mechanism of $YBa_2Cu_3O_x$ Films by TFA Metal-Organic Decomposition. *Chemistry of Materials,* Vol.18, No.26, (December 2006), pp. 6211-6219, ISSN 0897-4756

Schaf, J., Vieira, V., & Silva, J. (2001). Irreversibility limits of the Abrikosov and Josephson flux dynamics in homogeneous and granular high-T_C superconductors. *Physical Review B,* Vol.64, No.9, (August 2001), pp. 094516-1-7, ISSN 1098-0121

Schaf, J., & Vieira, V. (2002). Anisotropic irreversibility of the Abrikosov and Josephson flux dynamics in $YBa_{2-x}Sr_xCu_3O_{7-\delta}$ single crystals: Bose-glass and vortex-glass features. *Physical Review B,* Vol.65, No.14, (April 2002), pp. 144531-1-9, ISSN 1098-0121

Schaf, J., Pureur, P., & Vieira, V. (2002). Effects of Zn and Mg in Cu sites of $YBa_2Cu_3O_{7-\delta}$ single crystals on the resistive transition, fluctuation conductivity, and magnetic irreversibilities. *Physical Review B,* Vol.66, No.22, (December 2002), pp. 224506-1-11, ISSN 1098-0121

Schaf, J., Pureur, P., Dias, F., Vieira, V., Rodrigues Jr., P., & Obradors, X. (2008). Correlation between the magnetic irreversibility limit and the zero resistance point in different granular $YBa_2Cu_3O_{7-\delta}$ superconductors. *Physical Review B,* Vol.77, No.13, (April 2008), pp. 134503-1-8, ISSN 1098-0121

Stroud, D., Ebner, C., & Shih, W. (1984). Frustration and disorder in granular superconductors. *Physical Review B,* Vol.30, No.1, (July 1984), pp. 134-144, ISSN 1098-0121

Vinokur, V., Kes, P., & Koshelev, A. (1990). Flux pinning and creep in the very anisotropic high temperature superconductors. *Physica C,* Vol.168, No.1-2, (June 1990), pp. 29-39, ISSN 0921-4534

Yeshurun, Y., & Malozemoff, A. (1988). Giant flux creep and irreversibility in an Y-Ba-Cu-O crystal: an alternative to the superconducting-glass model. *Physical Review Letters,* Vol.60, No.21, (May 1988), pp. 2202-2205, ISSN 0031-9007

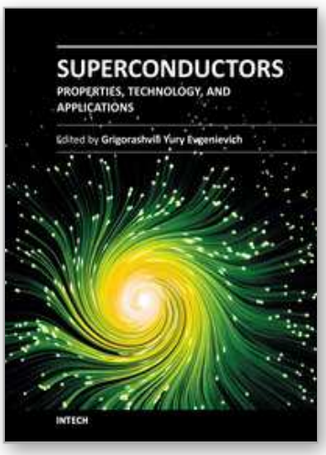

Superconductors - Properties, Technology, and Applications
Edited by Dr. Yury Grigorashvili

ISBN 978-953-51-0545-9
Hard cover, 436 pages
Publisher InTech
Published online 20, April, 2012
Published in print edition April, 2012

Book "Superconductors - Properties, Technology, and Applications" gives an overview of major problems encountered in this field of study. Most of the material presented in this book is the result of authors' own research that has been carried out over a long period of time. A number of chapters thoroughly describe the fundamental electrical and structural properties of the superconductors as well as the methods researching those properties. The sourcebook comprehensively covers the advanced techniques and concepts of superconductivity. It's intended for a wide range of readers.

InTech Europe
University Campus STeP Ri
Slavka Krautzeka 83/A
51000 Rijeka, Croatia
Phone: +385 (51) 770 447
Fax: +385 (51) 686 166
www.intechopen.com

InTech China
Unit 405, Office Block, Hotel Equatorial Shanghai
No.65, Yan An Road (West), Shanghai, 200040, China
中国上海市延安西路65号上海国际贵都大饭店办公楼405单元
Phone: +86-21-62489820
Fax: +86-21-62489821

IntechOpen